Sleep Medicine Reviews 59 (2021) 101495

Contents lists available at ScienceDirect

Sleep Medicine Reviews

journal homepage: www.elsevier.com/locate/smrv

CLINICAL REVIEW

Structural and functional magnetic resonance imaging in isolated REM sleep behavior disorder: A systematic review of studies using neuroimaging software

Anna Campabadal [a, b], Barbara Segura [a, b, c], Carme Junque [a, b, c, *], Alex Iranzo [b, c, d]

[a] Medical Psychology Unit, Department of Medicine, Institute of Neuroscience, University of Barcelona, Barcelona, Catalonia, Spain
[b] Institute of Biomedical Research August Pi i Sunyer (IDIBAPS), Barcelona, Catalonia, Spain
[c] Centro de Investigación Biomédica en Red Sobre Enfermedades Neurodegenerativas (CIBERNED:CB06/05/0018-ISCIII), Barcelona, Spain
[d] Sleep Disorders Center, Neurology Service, Hospital Clínic, Barcelona, Catalonia, Spain

ARTICLE INFO

Article history:
Received 10 February 2021
Received in revised form
8 April 2021
Accepted 12 April 2021
Available online 22 April 2021

Keywords:
Isolated REM sleep behavior disorder
Neuroimaging
MRI
Biomarkers
fMRI
REM sleep
Prodromal Parkinson's disease

SUMMARY

Isolated rapid eye movement sleep behavior disorder (iRBD) is a harbinger for developing clinical synucleinopathies. Magnetic resonance imaging (MRI) has been suggested as a tool for understanding the brain bases of iRBD and its evolution. This review systematically analyzed original full text articles on structural and functional MRI in patients with video-polysomnography-confirmed iRBD according to systematic procedures suggested by Reviews and Meta-analyses (PRISMA). The literature search was conducted via the PubMed database for articles related to structural and functional MRI in iRBD from 2000 to 2020. Investigations to date have been diverse in terms of methodology, but most agree that patients with iRBD have structural changes in deep gray matter nuclei, cortical gray matter atrophy, and disrupted functional connectivity within the basal ganglia, the cortico-striatal and cortico-cortical networks. Furthermore, there is evidence that MRI detects structural and functional brain changes associated with the motor and non-motor symptoms of iRBD. The current review highlights the need for larger multicenter and longitudinal studies, using complex approaches based on data-driven and unsupervised machine learning that will help to identify structural and functional patterns of brain degeneration. In turn, this may even allow for the prediction of subsequent phenoconversion from iRBD to the clinically defined synucleinopathies.

Rationale and objectives

Rapid eye movement (REM) sleep behavior disorder (RBD) is a parasomnia characterized by a loss of normal skeletal muscle atonia during REM sleep that leads to prominent motor activity and unpleasant dreaming (American Academy of Sleep Medicine, 2014). The pathogenesis is thought to be related to dysfunction of the lower brainstem nuclei that regulates muscle atonia during REM sleep [1]. Evidence suggests that isolated RBD (iRBD) is a prodromal stage of the various clinically defined synucleinopathies, with 90% of patients having abnormal synuclein in their cerebrospinal fluid [2]. These patients typically progress to Parkinson's disease (PD), dementia with Lewy bodies (DLB), and rarely, multiple system atrophy (MSA) after 15 years of follow-up [3]. Thus, it is reasonable to expect dysfunction in structures other than the brainstem nuclei to be present during the evolution of this disorder, including regions such as the striatum, the substantia nigra (SN), the limbic system, and the cortex, which may indicate a widespread neurodegenerative process.

In this context, there is a need to detect biomarkers of neurodegeneration in iRBD to help explain the underlying pathogenesis and predict the short-term risk of conversion to PD, DLB, or MSA. Several clinical, genetic, and neuroimaging biomarkers of neurodegeneration have been identified in iRBD that point toward alterations in the brainstem and other areas. Among the various neuroimaging markers, nuclear medicine is the best-known technique and is used most widely across the world to study brain changes associated with iRBD. The results of these nuclear medicine approaches have been extensively reviewed in prior work [4].

* Corresponding author. Medical Psychology Unit, Department of Medicine, University of Barcelona, Casanova 143, 08036, Barcelona, Spain. Fax: +34 93 403 52 94.
E-mail address: cjunque@ub.edu (C. Junque).

https://doi.org/10.1016/j.smrv.2021.101495

Abbreviations

AD	axial diffusivity
ALFF	amplitude of low-frequency fluctuations
BG	basal ganglia
BOLD	blood oxygen level-dependent
DLB	dementia with Lewy bodies
DTI	diffusion tensor imaging
FA	fractional anisotropy
FC	functional connectivity
GM	gray matter
HC	healthy controls
iRBD	idiopathic REM sleep behavior disorder
MD	mean diffusivity
MRI	magnetic resonance imaging
MSA	multiple system atrophy
PD	Parkinson's disease
RBD	REM sleep behavior disorder
RD	radial diffusivity
ReHo	regional homogeneity
rs-fMRI	resting-state functional MRI
SN	substantia nigra
UPDRS	the unified Parkinson's disease rating scale
VBM	voxel-based morphometry
WM	white matter

Although there has been less study into magnetic resonance imaging (MRI), to date this has demonstrated the capability to detect regional brain abnormalities associated with the early neurodegenerative process in iRBD, so much so that some have proposed using MRI to assess prodromal brain changes in synucleinopathies. As with nuclear medicine imaging, MRI can focus on both regions related to RBD and on regions that have previously been reported in neuroimaging studies of PD, DLB, and MSA. Novel MRI techniques could therefore help with the monitoring of disease progression and with the identification of subsequent phenoconversion risk in these patients, allowing for their inclusion in clinical trials of drugs with neuroprotective potential. Although still insufficient, there is a growing literature base regarding the brain changes associated with iRBD on structural and functional MRI.

In the present work, we aimed to conduct a systematic review of original full text articles that have used neuroimaging software analysis of structural and functional MRI in patients with video-polysomnography-confirmed iRBD, and to disentangle their relationship with clinical variables such as cognition. Furthermore, we discuss how differences in sample composition and the neuroimaging methodological approaches have influenced the discrepancies among studies.

Search strategies, selection criteria and data extraction process

This review adopted the relevant criteria of the preferred reporting items for systematic reviews and meta-analyses (PRISMA). The literature search was conducted via the PubMed database in November 2020 for articles related to structural and functional MRI studies in iRBD. We used the terms and combinations listed in Table S1, filtered for the period from 2000 to 2020. After removing duplicates, as well as screening the titles, abstracts, and/or full texts for suitability, we excluded 1476 studies. Details of the steps of database search are given in Fig. 1. The following criteria were then applied for inclusion in the review: 1) original articles; 2) English full text available; 3) iRBD diagnosis confirmed by video-polysomnography; 4) case–control studies that included patients with iRBD; 5) structural and functional MRI studies that used neuroimaging software analysis. This resulted in 27 full text articles being included for the final review. Two reviewers independently screened all articles identified from the search. First, all titles and abstracts of the articles returned from initial searches were screened based on the inclusion criteria. Next, full texts were examined in detail for applicability. If the relevance of an abstract was unclear, it was reviewed with full-text screening. Any disagreement between reviewers was resolved by discussion to meet a consensus. The other two reviewers were consulted to decide if consensus is not achieved initially.

The following information from each included study was extracted: 1) author(s); 2) year of publication; 3) source of data; 4) follow-up period; 5) sample size; 6) demographic data; 7) contrasts; 8) MRI modalities; 9) neuroimaging features; and 10) data analysis techniques.

Structural MRI studies in iRBD

Different MRI techniques have been used to assess gray matter (GM) abnormalities in patients with iRBD, such as voxel-based morphometry (VBM), vertex-based shape analysis, cortical thickness, and deep GM volumetry. Given that the basal ganglia (BG) are implicated in parkinsonism and that iRBD appears to be a harbinger of synucleinopathies, research into iRBD initially focused on the striatum. Subsequently, interest has broadened toward the study of GM beyond the striatal regions, including cortical GM and white matter (WM) areas that have also been reported to be affected in parkinsonism. Table 1 presents the studies showing structural changes in iRBD.

Deep GM changes in iRBD

Over the last decade, volumetric and VBM works have consistently identified reduced volume in the putamen [5,6] and caudate nucleus [5,7] in people with iRBD relative to HC. This finding supports the results of dopamine transporter single-photon emission computed tomography studies that have highlighted the existence of presynaptic dopaminergic dysfunction [8], with the degree of damage determining conversion to PD and DLB. Furthermore, patients with iRBD have showed volume reductions in the external and internal left pallidum [5] as well as the cerebellum [9], when studied by shape analysis and VBM, respectively. Regarding the thalamic nuclei, another structure implicated in the sleep–week cycle [1], results are still controversial. While some works have found that there is a reduced volume [48], others have reported increased GM volume in such structure [7,10] using VBM, shape analysis and volumetry techniques. Since the thalamus is a complex structure, additional approaches that use thalamic segmentation [11] may shed light on the roles of specific thalamic nuclei in iRBD.

Atrophy of the hippocampus and related structures has previously been reported in DLB [12,13], PD with hallucinations, and PD with dementia [14], and as such, could represent a biomarker of neurodegeneration in iRBD. Nevertheless, there is uncertainty on this matter because both increased [15] and decreased [16] hippocampal volumes, as well as parahippocampal gyrus volumes [9], have been reported in iRBD when studied with VBM [9,15], shape

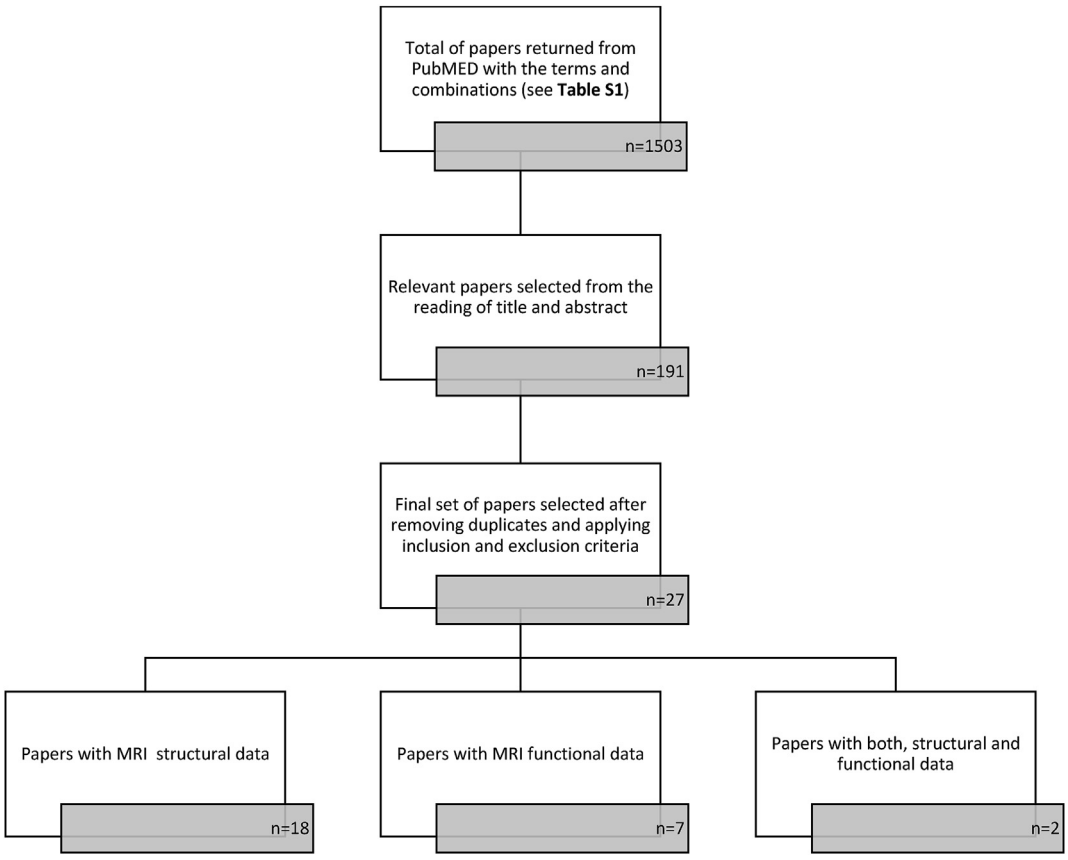

Fig. 1. Flow diagram describing the details of the steps of database search.

analysis and segmentation [16] techniques. A recent study using shape analysis showed a volume reduction in the right posterior hippocampus in patients with iRBD relative to HC [16]. Specifically, the hippocampal subfield segmentation revealed that the iRBD group had greater atrophy in the right CA1 and CA4 subfields, molecular layer, and granule cell layer of the dentate gyrus [16] consistent with previous findings in DLB and PD [12,13,17,18]. The exploratory nature of the hippocampal subfield data in this work [16] necessitates that these results be confirmed in larger samples.

The suspected pathophysiology of RBD is that there is an underlying dysfunction of the lower brainstem nuclei that modulates REM sleep muscle tone [1]. In two VBM studies, volume reductions have been reported in these structures compared to HCs [9,19]. Hanyu et al. (2012) [9] identified GM reductions in the tegmental portion of the pons, a region that has a role in sleep stage regulation. While investigation of the brainstem by MRI has been hampered for years due to the physiological and anatomical characteristics of this brain structure, there have been significant advances in recent years thanks to the broader adoption of ultrahigh field MRI scanning (7 T and higher) [20]. Knowledge of specific brainstem regions involved in iRBD should improve with increased access to this technology.

There is a broad consensus that patients with iRBD have deep GM volume reductions. However, only a few studies have identified volume increases in the hippocampus [15], cerebellum [7,21], thalamus [7,10], and striatum [7,10,21]. Some authors of these reports have suggested that the volumetric increases may reflect a compensatory effect [7,21]. Irrespective, the discrepancies with most of the studies could be explained by their small samples, and particularly in the multicenter study by Holtbernd et al. (2020) [21], the lack of an MRI homogenization protocol.

Ellmore et al. (2010) [6] was the first to compare patients with iRBD to age-matched patients with early PD. Surprisingly, they found that the iRBD group had significantly smaller left putamen through subcortical volumetry. Consistent with earlier suggestions in studies comparing iRBD and HC groups, the authors suggested that the dopaminergic decease may be related to compensatory increase in striatal volume. However, only two works have studied the differences between iRBD and PD since then, rendering any debate preliminary. In the multicenter study by Holtbernd et al., (2020) [21], thalamic volume was noted to be reduced bilaterally in patients with iRBD compared to those with PD using tensor-based morphometry, while brainstem and cerebellum volumes were increased. In contrast to these findings, recent work using structural MRI from the Parkinson's progression markers initiative database found no differences in subcortical measures between patients with de novo PD and patients with iRBD [22]. The authors suggested that the lack of a significant difference could be due to a high prevalence of future iRBD to PD converters in their sample, meaning that subtle PD-like deep GM changes were already present in patients with iRBD. The heterogeneity of iRBD may preclude finding consistent reductions in deep GM volume. Further multicenter studies are therefore needed.

Cortical GM changes in iRBD

Although the pathophysiology of iRBD is centered on the brainstem nuclei, good evidence supporting the existence of neocortical neurodegeneration in PD, DLB, and MSA has prompted research into possible cortical changes in iRBD. It has been shown that, compared with HC, patients with iRBD have cortical thinning in the lingual gyrus [23], fusiform gyrus [16,23], lateral occipital

Table 1
Studies of structural MRI in iRBD. Only those contrasts involving the iRBD group are included. Demographics are presented as, age; disease duration in y±SD.

Reference	Sample	Demographics	MRI analysis	Contrast	Brain regions
MRI structural imaging					
Campabadal et al., 2019 [16]	20 iRBD 27 HC	71.3 ± 7.8; 3.1 ± 3.5 66.4 ± 9.9	CTh SB vol Shape analysis Subfield segmentation (hippocampus)	iRBD<HC	- Cortical thinning in the R superior frontal, L postcentral and L superior parietal, L fusiform gyrus, and R lateral occipital - ⇩volume in the R hippocampus. - ⇩surface in the R posterior hippocampus ⇩volume in the R CA1, molecular layer, granule cell layer of the dentate gyrus, and CA4
Campabadal et al., 2020[b] [24]	14 iRBD 18 HC	70.1 ± 6.9; 4.5 ± 3.4 68.3 ± 7.5	CTh SB vol	iRBD effect time	Cortical thinning in the L superior parietal, lateral orbitofrontal and precentral, and the R rostral middle frontal, superior frontal and inferior parietal
				Group by time (iRBD<HC)	Cortical thinning bilaterally in the superior parietal and the L lateral orbitofrontal
Chen et al., 2020 [7]	27 iRBD 33 HC	65.9 ± 8.5; 11.1 ± 11.2 68.3 ± 7.8	VBM	iRBD<HC	⇩volume bilaterally the temporal poles and middle occipital gyri, R caudate, superior frontal, supramarginal and middle temporal gyri, and L inferior orbitofrontal gyri, supplementary motor area and cerebellar crus
				iRBD>HC	⇧volume bilaterally cerebellum, thalamus, putamen, L superior occipital, precentral and R inferior occipital gyri
Ellmore et al., 2010 [6]	5 iRBD 5 PDnovo 7 HC	52.6 ± 10.1; n.a. 60.0 ± 9.6; n.a. 54.0 ± 7.8	SB vol	iRBD<HC	⇩volume in bilateral putamen
				iRBD< PDnovo	⇩volume in L putamen
Hanyu et al., 2012 [9]	20 iRBD 18 HC	68 ± 7; 6 ± 5 71 ± 8	VBM (1.5T)	iRBD<HC	⇩volume in R and L anterior lobes of the cerebellum, tegmental portion of the pons and L parahippocampus
Holtbernd et al., 2020[a] [21]	30 iRBD 29 PD 56 HC	66.8 ± 9.1; 10.1 ± 13.5 63.5 ± 8.3; 6.7 ± 7.1 62.9 ± 11.0	CTh TBM (ROIs cortical GM, WM, DGM, cerebellum, brainstem)	iRBD>HC	⇧volume R caudate and cerebellum (cerebellar crus I, lobule X and cerebellar WM)
				iRBD = HC<PD	⇩volume bilateral thalamus
				iRBD>PD	⇧volume in the brainstem (the locus coeruleus, medulla oblongata, reticular formation and the pons) and cerebellum (lobules I–V, VIIb, VIIIa/b, IX, X, Crus I, and cerebellar WM)
Lee et al., 2014 [64]	15 iRBD 20 HC	62.8 ± 7.4; 5.9 ± 3.2 60.0 ± 6.4	VBM SB vol	iRBD>HC	⇧lateral ventricle volume
Li et al., 2020 [19]	32 iRBD 33 HC	64.9 ± 7.7; n.a. 63.3 ± 5.3	VBM (5 ROIs of the central autonomic network)	iRBD<HC	⇩volume in the brainstem, anterior cingulate and insula
Park et al., 2018 [10]	10 iRBD 14 HC	67.0 ± 6.4; n.a. 67.2 ± 4.5	GM volumetry	iRBD<HC	⇩volume L pars opercularis, R isthmus cingulate cortex
				iRBD>HC	⇧volume R lateral orbitofrontal, rostral middle frontal and caudate, and bilateral thalami
Pereira et al., 2019[b],[a] [22]	27 iRBD[a] - 21 iRBDnc	68.9 ± 5.5; n.a. - 69.2 ± 5.9; n.a.	CTh SB vol	iRBD<HC	Cortical thinning in the L lateral occipital, postcentral gyri,

Table 1 (*continued*)

Reference	Sample	Demographics	MRI analysis	Contrast	Brain regions
	- 6 iRBDc 151 PDnovo 31 HC	- 67.8 ± 4.1; n.a. 60.6 ± 9.6; <2 58.5 ± 11.0			inferior parietal and supramarginal areas
				iRBDc<HC (at baseline)	Cortical thinning in the bilateral frontal, precentral and occipital cortices
				iRBDc<iRBDnc (at baseline)	Cortical thinning in L superior frontal, R precentral and lateral occipital gyri
Rahayel et al., 2015 [23]	24 iRBD 42 HC	64.2 ± 7.0; 9.3 ± 9.0 63.3 ± 7.1	Cth VBM	iRBD<HC	Cortical thinning in the R medial frontal (cingulate, paracingulate and gyrus rectus), the R dorsolateral superior frontal, the lingual and fusiform gyri ⇩volume in the R superior frontal sulcus
Rahayel et al., 2018 [5]	41 iRBD 41 HC	65.2 ± 6.4; 12.0 ± 12.7 63.4 ± 9.0	CTh VBM Shape analysis SB vol	iRBD<HC	Cortical thinning in the bilateral medial superior frontal, orbitofrontal, anterior cingulate cortices and the R dorsolateral primary motor cortex ⇩volume in the anterior cingulate, the orbitofrontal and gyrus rectus, the L primary motor and premotor cortices, L anterior dorsolateral prefrontal cortex, the R superior frontal sulcus and the R caudate ⇩surface in the L pallidum ⇩volume in R putamen
Rahayel et al., 2018 [48]	17 iRBD-MCI 35 iRBD-NMCI 41 HC	67.9 ± 4.4; 12.6 ± 13.3 64.4 ± 7.2; 11.2 ± 11.3 63.2 ± 8.2	CTh VBM Shape analysis	iRBD-MCI<HC	Cortical thinning in the bilateral anterior temporal lobe and insula, the L entorhinal cortex, posterior temporal lobe, the L fusiform cortex, bilateral superior medial frontal, L inferior and middle frontal cortices, the L paracentral, bilateral anterior cortices and the L posterior cingulate cortex ⇩volume in precentral and postcentral cortex ⇩surface L pallidum and bilateral putamen and thalamus
				iRBD-NMCI<HC	Cortical thinning in the bilateral paracentral, R precentral cortex and L superior medial frontal
				iRBD-MCI< iRBD-NMCI	Cortical thinning bilaterally in the insula, the L anterior and posterior temporal lobes, including the L fusiform, and lingual gyri, and the R middle temporal gyri, the L lateral occipital cortex, the L medial superior frontal, and R superior frontal and bilateral posterior cingulate, and L anterior cingulate ⇩surface in the L putamen and thalamus
Scherfler et al., 2011 [15]	26 iRBD 14 HC	67.4 ± 4.9; 9.2 ± 6.4 64.5 ± 5.2	VBM (1.5T)	iRBD>HC	⇧bilateral hippocampi
Diffusion tensor imaging					
Holtbernd et al., 2020[a] [21]	23 iRBD 23 PD 53 HC	n.a.	DTI (ROIs cortical GM, WM, DGM, cerebellum, brainstem)	iRBD>HC	⇧FA in the bilateral SN, red nuclei, pedunculopontine nuclei, dorsal and medial raphe nuclei, locus coeruleus, the medulla oblongata, the reticular

(*continued on next page*)

Table 1 (*continued*)

Reference	Sample	Demographics	MRI analysis	Contrast	Brain regions
					formation, and the bilateral inferior, middle and superior cerebellar peduncles, and in both corticospinal tracts, R superior longitudinal fasciculus and anterior thalamic radiation, and the L uncinate fasciculus
				iRBD = PD<HC	⇩FA in the corpus callosum
				iRBD>PD	⇧FA in the bilateral SN, R red nuclei, pedunculopontine nuclei, dorsal and medial raphe nuclei, locus coeruleus, the medulla oblongata, and the superior cerebellar peduncles and the R inferior cerebellar peduncle
Ohlhauser et al., 2019[a] [36]	20 proPD (14 iRBD) 17 PDnovo 21 HC	68.0 ± 5.9; n.a. 67.7 ± 6.0; n.a. 68.2 ± 4.7	DTI	iRBD>PDnovo	⇧MD corpus callosum, R internal/external capsule, superior and inferior longitudinal fasciculus, the corticospinal tract, forceps major, corona radiata
Pyatigorskaya et al., 2017 [35]	19 iRBD 18 HC	67.3 ± 8.0; 5.7 ± 3.8 66.5 ± 5.1	DTI (SN manual segmentation)	iRBD<HC	⇩FA in the SN
Scherfler et al., 2011 [15]	26 iRBD 14 HC	67.4 ± 4.9; 9.2 ± 6.4 64.5 ± 5.2	DTI (1.5T)	iRBD<HC	⇩FA mesencephalic tegmentum and the rostral pons
				iRBD>HC	⇧MD pontine tegmentum and reticular formation
Unger et al., 2010 [34]	12 iRBD 12 HC	59.0 ± 10.5; n.a. 56.8 ± 10.6	DTI (1.5T)	iRBD<HC	⇩AD pons, bilateral corona radiata and R SN ⇩FA Fornix, the R visual stream, and the L superior temporal lobe
				iRBD>HC	⇧FA bilateral internal capsule and olfactory regions ⇧RD fornix, the R visual stream, and the L superior temporal lobe
Structural connectivity					
Park et al., 2018 [10]	10 iRBD 14 HC	67.0 ± 6.4; n.a. 67.2 ± 4.5	Graph analysis (60 cortical and 13 subcortical regions)	iRBD<HC	⇩average degree, global efficiency and local efficiency ⇩BC R pars orbitalis
				iRBD>HC	⇧Characteristic path length ⇧BC bilateral caudate and several regions in the frontal cortex (bilateral caudal middle frontal, the L lateral orbitofrontal and superior frontal cortex, and the R pars triangularis, and rostral middle frontal cortex)

Abbreviations: AD, axial diffusivity; BC, betweenness centrality; CA, cornus ammonis; Cth, cortical thickness; DGM, deep gray matter nuclei; DTI, Diffusion-tensor imaging; FA, fractional anisotropy; GM, gray matter; HC, healthy control; iRBD, isolated REM sleep behavior disorder; iRBDc, iRBD that converted to a Lewy body disorder; iRBD-MCI, iRBD with mild cognitive impairment; iRBDnc, iRBD that did not phenoconvert; iRBD-NMCI, iRBD without mild cognitive impairment; L, left; MD, mean diffusivity; n.a., not available; NBS, network-based statistics; PD, Parkinson's disease; PDnovo, PD de novo patients; proPD, prodromal PD patients; R, right; RD, radial diffusivity; ROI, region of interest; SB vol, subcortical volumetry; SN, substantia nigra; TBM, tensor-based morphometry; VBM, voxel-based morphometry; WM, white matter.

[a] Some or all participants were extracted from the PPMI data (https://www.ppmi-info.org).

[b] Longitudinal study.

cortex [16,22], orbitofrontal cortex [5,23], cingulate cortex [5,23], and dorsolateral frontal cortex [5,23]. Atrophy of the parietal cortex is also present in iRBD, notably in the postcentral gyri [16,22] and the superior parietal cortex [16,24]. Other studies using whole brain voxel-based techniques have revealed decreased GM volumes in frontal [5,7,10,23], cingulate [5,10,19], occipital and parietal [7], and temporal regions [7,19]. Most studies of VBM and cortical thickness have found evidence of both anterior and posterior cortical degeneration in iRBD. Of note, after considering the sample size increase in Rahayel's works [5,23], the cortical involvement becomes predominantly anterior. This finding could be explained by the increase in disease duration, with the authors relating a

longer RBD duration and younger age of onset to GM atrophy primarily in anterior regions [5]. Another possibility is that introducing new cases of iRBD made the group less homogeneous (e.g., Rahayel et al., 2015 and 2018) [5,23] because there may have initially been a higher percentage of patients with prodromal DLB. Given this and the fact that cohorts with iRBD will include subjects in the prodromal stages of different synucleinopathies, it would be intriguing to identify patterns of cortical involvement with multicentric data and through more complex approaches based on data-driven and unsupervised machine learning. Such work has been undertaken with success for other neurodegenerative disorders [25–29]. Of greater interest would be the detection of specific cortical patterns that can highlight patients who will convert to PD or DLB.

Longitudinal data are now generating considerable interest. Despite decades of research, few works have examined structural brain markers that enable us to predict who will convert to a clinically defined synucleinopathy. Manifesting the typical morphological changes of MSA on conventional MRI has been suggested to have predictive power for phenoconversion in patients with iRBD [30], and as such, quantitative MRI analyses could confirm these preliminary data. Pereira et al. (2019) [22], investigated differences in cortical degeneration between patients with iRBD who converted a Lewy body disorder and those who did not over approximately 3 years. Using the baseline MRI images, they found that converters had widespread thinning in the left superior frontal, right precentral, and right lateral occipital gyri compared with non-converters. This work is of high relevance in understanding the MRI changes that distinguish the progression from iRBD to a clinically defined synucleinopathy, and effectively showed that mean cortical thickness predicted conversion with a hazard ratio of 0.784 (sensitivity of 95.2%, specificity of 100%, and area under the curve of 0.984). Nevertheless, the analyses were based on a small sample of converters (PD converters = 3; DLB converters = 1; MSA converters = 1; nonspecific parkinsonism converters = 1) precluding to investigate different brain atrophy patterns among specific iRBD progression. This will necessitate replication in larger samples. It should also be considered a limitation that this study did not include MRI follow-up for the HC group, which prevented us from accounting for the effects of aging.

Comparing the differential evolution in HC and iRBD, the latter has been reported to experience greater degeneration in the superior parietal and precuneus, the right cuneus, the left occipital pole, and a cluster involving the left lateral orbitofrontal and frontopolar cortices [24]. This pattern of cortical degeneration over time is similar to that previously described for PD and DLB [26,31–33]. Taking into account the results of the previous studies and in the absence of longitudinal studies based on other structural approaches, cortical thickness could be considered a sensitive measure of MRI changes in iRBD and its progression. Therefore, cortical thickness could be a structural marker of phenoconversion. Future prospective studies using this approach will help to identify whether a patient will eventually convert to PD, DLB, or MSA.

Diffusion tensor imaging

Diffusion tensor imaging (DTI) is a method that allows for the study of in-vivo microstructural brain tissue integrity based on diffusion restriction of water molecules. Most DTI investigations commonly use fractional anisotropy (FA) or radial (RD), mean (MD), or axial (AD) diffusivity, to provide insights into pathophysiological mechanisms. The first investigation to explore diffusivity in GM structures by whole brain analysis revealed that, relative to HC, those with iRBD exhibit decreased AD in the pons and the SN, as well as bilateral FA increases in the internal capsule and olfactory regions. By contrast, the left superior temporal lobule had both reduced FA and increased RD [34]. Subsequent investigations have identified reduced FA in the mesencephalic tegmentum, the rostral pons [15], and the SN [35], together with increased MD in the pontine tegmentum [15].

As mentioned, DTI is mostly used to provide information about microscopic changes in WM tissue, with evidence of decreased AD in the corona radiata [34], reduced FA and increased RD in the fornix and the right visual stream [34], and increased MD in the reticular formation [15]. Notably, Ohlhauser et al. (2019) [36] studied a cohort with prodromal PD (RBD and/or hyposmic patients) relative to those with de novo PD. The authors found that patients with iRBD had increase MD in the corpus callosum, internal and external capsule, the superior and inferior longitudinal fasciculus, the corticospinal tract, the forceps major, and the corona radiata relative to de novo PD. One might therefore speculate that iRBD represent a unique clinical subtype of progression that has a more severe prognosis due to the greater extent of brain atrophy.

Decreases in FA and increases in MD are interpreted as an alteration in brain microstructure integrity. However, increased FA in the WM has also been reported in some neurodegenerative disorders, possibly reflecting a gain of myelination and loss of dendrite sprouting and glial cell activation [37]. Accordingly, a study using diverse regions of interest uncovered increased FA in deep GM structures in patients with iRBD [21]. Similar to the volumetric data, the methodological differences between studies mean that care is necessary when comparison data sets. Nevertheless, these studies demonstrate that the presence of iRBD is associated with microstructural abnormalities in regions that regulate REM sleep, as well as in structures that have known associations with neurodegenerative pathology in PD.

Structural connectivity

Structural connectivity refers to the existence of connections between different brain regions, usually derived from diffusion-weighted imaging through tractography. Less frequently, GM atrophy measures derived from T1-weighted MRI are used to build connectivity matrices based on the correlation coefficient between paired regions. Unfortunately, although there have been some studies of structural connectivity in prodromal PD [38,39], only one preliminary work has used this approach in a exclusively sample of patients with iRBD [10].

In the research by Park et al. (2018) [10], the authors used T1-weighted images to define 73 regions of interest and obtained partial correlation matrices between every pair of nodes. They finally computed graph analysis parameters that manifests topological disorganization of the global brain network including decreased global network, average degree, global efficiency, and local efficiency, and increased characteristic path length in patients with iRBD in comparison to HC. Furthermore, they found both reduced and increased betweenness centrality, a measure of the importance of individual nodes in a given network, in several regions in the frontal cortex and bilaterally in the caudate nucleus. The main limitation of this work was its small sample size of 10 patients with iRBD and the persistent controversy over the use of T1-weighted images to study structural connectivity. Some authors argue that GM structural connectivity cannot be considered a direct measure of connectivity, unlike the DTI approach, while others consider that this approach provides additional insights into the brain network topographical organization [40]. Given evidence that WM changes can be shown with DTI approaches and that structural connectivity research is possible through diffusion MRI tractography, this is a promising field that requires further investigation with larger iRBD cohorts.

Table 2
Studies of functional MRI in iRBD. Only those contrasts involving the iRBD group are included. Demographics are presented as, age; disease duration in y±SD.

Reference	Sample	Demographics	MRI analysis	Contrast	Brain regions
Byun et al., 2020 [45]	37 iRBD 15 HC	67.7 ± 7.1; 6.8 ± 3.8 68.3 ± 3.3	Seed-to-voxel analysis (Thalamo-cortical FC)	iRBD>HC	⇧FC between the L thalamus and occipital regions (R cuneus, L fusiform and lingual gyri)
Campabadal et al., 2020 [47]	20 iRBD 27 HC	71.0 ± 10.0; 2.0 ± 5.0 66.5 ± 13.0	Whole brain (TFNBS) and graph analysis	iRBD<HC	⇩cortico-cortical FC in posterior regions (including associative regions of the temporal and parietal lobes) ⇩BC L superior parietal
Chen et al., 2020 [7]	27 iRBD 33 HC	65.9 ± 8.5; 11.1 ± 11.2 68.3 ± 7.8	ALFF	iRBD>HC	⇧ALFF values in the R parahippocampal gyrus
Ehgoetz et al., 2020 [52]	30 iRBD 28 HC	66.7 ± 7.2; n.a. 65.6 ± 8.1	Task-based fMRI: event-related and seed-based approach (31 cortical and subcortical ROIs)	iRBD<HC (High vs Low load)	- ⇩BOLD signal in the dorsal caudate when dual-tasking in high versus low cognitive load ⇩FC between the motor network and striatum, and between the cerebellum and dorsal lateral prefrontal cortex
				iRBD>HC (High vs Low load)	⇧FC between the putamen and mesencephalic motor region
Ellmore et al., 2013 [42]	10 iRBD 11 PD 10 HC	57.0 ± 2.7; n.a. 62.0 ± 2.5; n.a. 57.0 ± 2.4	Seed-to-whole brain (bilateral SN as seeds)	PD<iRBD<HC	⇩FC between L SN and L putamen
				PD<iRBD>HC	⇧FC between R SN and R cuneus/precuneus
				PD>iRBD>HC	⇩FC between R SN and R superior occipital gyrus
Li et al., 2020 [46]	15 iRBD 15 HC	64.3 ± 1.9; n.a. 64.8 ± 1.8	ReHo and ALFF analysis, whole brain, and seed-to voxel (caudate and putamen as ROIs)	iRBD<HC	⇩ReHo in bilateral putamen, pallidum, insula, lentiform nucleus and L amygdala
				iRBD>HC	⇧ReHo in the superior frontal gyrus
Li et al., 2020 [19]	32 iRBD 33 HC	64.9 ± 7.7; n.a. 63.3 ± 5.3	Seed-to-whole brain (5 ROIs of the central autonomic network)	iRBD<HC	⇩FC between the brainstem and posterior cerebellum, temporal lobe and anterior cingulate
Rolinski et al., 2016 [41]	26 iRBD 48 PD 23 HC	67.0 ± 7.7; 2.4 ± 2.1 67.0 ± 7.7; 1.8 ± 1.5 n.a.	Resting state network analysis (a previously developed template of the BG network generated from 80 HC)	iRBD = PD<HC	⇩coactivation within the BG network and with frontal regions (cingulate and paracingulate gyri, the orbital cortices and the inferior and middle frontal gyri)
				iRBD = PD<HC	⇩mean parameter estimate values within the caudate, pallidum, and anterior/ posterior putamen
Yamada et al., 2019 [51]	23 iRBD 20 HC	71.3 ± 4.2; iRBD-MMI 5.6 ± 3.9 & iRBD-nMI 4.7 ± 3.0 70.7 ± 3.6	ROI-to-ROI (sensorimotor regions)	iRBD-MMI<HC	⇩FC between the R/L anterior putamen and R superior parietal lobule; and between L caudate and R superior parietal
				iRBD-nMI<HC	⇩FC between bilateral putamen and R superior parietal
				iRBD-MMI>iRBD-nMI	⇧FC between the cerebellum and primary somatosensory and premotor cortices

Abbreviations: ALFF, amplitude of low-frequency fluctuations; BG, basal ganglia; BOLD, blood oxygen level-dependent; FC, functional connectivity; fMRI, functional MRI; HC, healthy controls; iRBD, isolated REM sleep behavior disorder; iRBD-MMI, iRBD with mild motor impairment; iRBD-nMI, iRBD without mild motor impairment; L, left; n.a., not available; PD, Parkinson's disease; R, right; ROI, region of interest; ReHo, regional homogeneity; SN, substantia nigra; TFNBS, Threshold-free network-based statistics.

Functional MRI studies in iRBD

Resting-state (rs) functional MRI (fMRI) connectivity methods are based on the temporal correlations of spontaneous blood oxygen level-dependent (BOLD) signal fluctuations between different brain areas. Because this allows for the interaction between brain regions to be studied without the constraints of a specific cognitive task, it makes it especially suitable for the study of functional connectivity in aging and in neurodegenerative disease. It is possible that rs-fMRI will help to explain subtle abnormalities, even in the initial stages of a disease. There are different approaches and levels of complexity in the study of functional connectivity, potentially ranging from the study of connectivity between two regions (seed-to-seed based analysis), to the study of whole brain connectivity using complex network approaches, such as graph analysis. Table 2 shows the main functional findings in patients with iRBD.

Preliminary research in this field was carried out less than a decade ago [41,42], when it focused on BG dysfunction as a hallmark of early PD. Initially, Ellmore et al. (2013) [42] investigated seed-to whole brain connectivity from bilateral SN seeds in iRBD and PD brains using rs-fMRI. Their results highlighted that patients with iRBD had reduced connectivity between the left SN and the left putamen in comparison to HC, but increased connectivity in comparison to patients with PD. Moreover, the iRBD group had higher connectivity than the HC or PD groups between the right SN and cuneus/precuneus; however, they also had higher connectivity than the HC group between the right SN and superior occipital

gyrus, but this was lower than in the PD group. The authors concluded that altered nigrostriatal and nigrocortical connectivity characterizes iRBD before motor impairment.

Soon after this initial research, Rolinski et al. (2016) [41] proposed a new approach to detect functional connectivity changes in an ad hoc defined BG network with rs-fMRI. They demonstrated that both iRBD and PD groups had reduced coactivation within the BG network compared to a HC group, but also between the BG and frontal regions. Remarkably, this abnormal BG network connectivity allowed both PD and iRBD to be differentiated from HCs with high sensitivity (95.8% and 96.2%) and specificity (73.9 and 78.3%) (AUROC = 0.90 and 0.92, respectively), raising the potential role of functional connectivity to detect early dysfunction in BG circuitry, even in premotor stages. This highlighted the potential for using BG functional connectivity as a biomarker of early BG malfunction, helping to identify at-risk patients [41]. In light of this evidence, rs-fMRI was considered a promising new biomarker of prodromal neurodegeneration in PD [43].

Most subsequent research on BG functional connectivity has followed the same line as these original studies, with some using other rs-fMRI approaches. For instance, Dayan and Browner (2017) [44] took a new look at BG dysfunction in prodromal PD for the study of BG connectivity as a network itself. This work included patients suffering iRBD and/or hyposmia, but because it focused on prodromal stages of PD, caution should be taken when generalizing their results to the iRBD population. This research revealed that, relative to HCs, the prodromal PD group had reduced striato-thalamo-pallidal functional connectivity. Other researchers have looked at thalamic functional connectivity beyond the striato-thalamo-pallidal circuitry using a seed-to-whole brain [45]. In this work, the authors reported increased connectivity relative to HC between the left thalamus and posterior regions in patients with iRBD, including the right cuneus cortex and the left fusiform and lingual gyri. More recently, while attempting to study functional connectivity changes in the central autonomic network, Li et al. (2020) [19] selected five regions as seeds (the brainstem, hypothalamus, amygdala, anterior cingulate, and insula), to compute independent seed-to-whole brain data. The results reflect the fact that the brainstem in iRBD had significantly reduced functional connectivity with the posterior cerebellum, left temporal lobe, and anterior cingulate. Although other approaches, such as network-based statistics, would have better characterized the dynamic interaction between the different brain regions, their data revealed disrupted brainstem functional connectivity in iRBD for the first time.

A major drawback of the aforementioned works is that they focused on previously selected regions, mainly the BG [41,42,45,46]. Although their approaches are fully justified on the assumption that iRBD is a prodromal stage of PD, this raises questions about functional whole brain connectivity in iRBD. Recently, using a whole brain analysis conducted by a complex network approach revealed that cortico-cortical connectivity is also reduced. Whole brain analysis was noted for showing decreased posterior cortico-cortical functional connectivity strength in patients with iRBD compared with HC. The results revealed disrupted connectivity in associative regions of the temporal and parietal lobes that are known to support complex cognitive functions. It is worth noting that functional disruption of the parietal cortex was also confirmed by a sophisticated graph analysis that identified decreased centrality for a node located in the left superior parietal lobule [47]. This finding might reflect the parietal cortex losing its role in integrating sensory and cognitive information, and it is supported by evidence of an association between neuropsychological dysfunction and abnormalities in this structure [22,24,47,48].

In contrast to functional connectivity, which characterizes the relationship between brain regions, amplitude of low-frequency fluctuations (ALFF) and regional homogeneity (ReHo) are two fMRI methodologies used to study more local spontaneous neuronal activity. To date, only two investigations have applied these approaches in iRBD cohorts. One of these uncovered an increase in ALFF values in the right parahippocampus [7]. The increased regional brain activity in the parahippocampus was consistent with findings from previous studies showing metabolic and perfusion abnormalities in this region [4]. The other research focused on the striatum and detected that patients with iRBD had significantly bilaterally decreased ReHo in the putamen [46]. When they broadened their analysis, whole brain results showed bilaterally decreased ReHo in the putamen, pallidum, insula, lentiform nucleus, and left amygdala, together with increased ReHo in the frontal cortex.

MRI correlates of clinical and neuropsychological data

MRI has proven to be a powerful tool for identifying brain structural and functional abnormalities underlying the features of iRBD. Table 3 summarizes the main clinical and neuropsychological correlates of iRBD on MRI.

Clinical and motor features

A longer duration of RBD and a younger age of estimated RBD onset have been associated with GM volume reduction in the frontal lobes, cortical thinning in the left medial superior frontal and supramarginal cortices, and thinning in the precuneus [5]. Longitudinal data indicate that patients with a late estimated onset of RBD had greater bilateral cortical loss in the precuneus and lateral occipital gyri after 1.6 years' follow-up [24]. In the same line, other iRBD severity measures have been correlated with structural and functional brain changes in iRBD [5,19,48–50].

As a prodromal state of parkinsonism, there is a growing interest in the study of motor status in iRBD. This is typically assessed with the motor component of the unified PD rating scale (UPDRS) or the international Parkinson and movement disorders society UPDRS (MDS-UPDRS). Increased scores in the UPDRS-III motor scale are related to smaller caudate and higher local GM cerebellar volumes [5], while increased scores in the MDS-UPDRS-III motor scale are related to higher cortical thinning in the superior frontal, precentral, and fusiform regions [22]. Of note, when motor output is assessed more thoroughly, slower finger tapping of the right hand was associated with cortical thinning in the right paracentral and superior parietal lobe cortices, shape contraction in the right putamen, and with bilateral shape contraction in the pallidum. By contrast, motor function in the left hand correlated with cortical thinning in the right postcentral and superior parietal cortices [5]. Only one investigation to date has studied this association using a longitudinal approach. Changes in motor signs measured by the MDS-UPDRS-III over time were related to bilateral cortical degeneration in superior parietal, left superior frontal, and right rostral middle frontal regions [24].

There have only been two studies into the motor status in iRBD assessed by fMRI with both using very different methodologies to assess functional connectivity (Table 2). Yamada et al. (2019) [51] showed increased connectivity between the cerebellum and primary somatosensory and premotor cortices underlying mild motor impairment in iRBD. They hypothesized that increased cerebellar-cortical functional connectivity may have reflected compensation for mild nigrostriatal dopaminergic dysfunction. However, this compensatory effect was questionable because the patients manifested mild motor impairment despite the connectivity increases. In the work by Ehgoetz Martens et al. (2020) [52], investigating the substrates underlying dual-task interference on gait in iRBD revealed BOLD signal reduction in the caudate nucleus when dual-tasking in

Table 3
The main clinical and neuropsychological MRI correlates of iRBD.

Reference	RBD duration	Olfaction	Motor status	FFEE/Attention	Visuospatial	Color	Memory
Byun et al., 2020 [45]							L thalamus- L fusiform FC
Campabadal et al., 2020 [24]			Longitudinal changes associated with ⇩ CTh bilaterally in superior parietal, L superior frontal, and R rostral middle frontal		⇩ CTh in bilateral superior parietal cortical regions		
Campabadal et al., 2020 [47]				⇩ FC between R superior parietal and L inferior temporal			
Campabadal et al., 2019 [59]		anosmic iRBD, ⇩ GM volume in orbitofrontal regions with a R predominance					
Chen et al., 2020 [7]		⇧ ALFF in R superior occipital gyrus					
Rahayel et al., 2018 [48]		⇩ CTh bilateral lateral occipital and R cuneus		⇩ CTh in the medial superior, dorsolateral paracentral, sensorimotor, fusiform, lingual, and cuneus	⇩ CTh in the frontal, temporal, posterior lingual and fusiform, insular, precuneus, and cuneus and lateral occipital ⇩ GM volume in the R lateral occipital ⇧ surface expansion R hippocampus	⇩ CTh in the R cuneus. Abnormal surface expansion R hippocampus	⇩ CTh in the temporal (pole, anterior superior, posterior lingual and fusiform), insular, and cuneus. ⇧ surface expansion R hippocampus
Rahayel et al., 2018 [5]	⇩ GM volume in the frontal cortices ⇩ CTh in the L medial superior frontal and supramarginal cortex and precuneus		⇩ caudate and ⇧ cerebellum volumes				
Pereira et al., 2019 [22]		⇩ CTh bilateral medial orbitofrontal and L precentral	⇩ CTh of the L superior frontal and fusiform and R precentral gyri		⇩ CTh L fusiform and R supramarginal		⇩ CTh in the L superior temporal, L caudal middle frontal, R superior frontal and R lateral occipital gyri

Abbreviations: ALFF, amplitude of low-frequency fluctuations; CTh, cortical thickness; FC, functional connectivity; FFEE, executive functions; GM, gray matter; iRBD, isolated REM sleep behavior disorder; L, left; R, right; RBD, REM sleep behavior disorder.

high versus low cognitive load. There were also functional connectivity disruptions between the motor network and the striatum and between the cerebellum and dorsal lateral prefrontal cortex. Although these studies are promising, there is still much work to be done, particularly concerning the functional changes that may indicate motor progression, and as such, may predict phenoconversion.

Neuropsychological data

Cognitive impairment has been systematically reported in iRBD [53]. In a study by Rahayel et al. [48], patients with iRBD who had additional mild cognitive impairment showed cortical thinning in the frontal, cingulate, temporal, the insular, and occipital cortices, and abnormal surface contraction in the putamen and thalamus, while those without impairment had cortical thinning restricted to the frontal cortex (Table 1). Thinning in the right middle temporal cortex discriminated patients with mild cognitive impairment from those with normal cognition (AUROC = 0.79). It is worth noting that, although they used both VBM and cortical thickness analyses, the latter was found to be more sensitive at detecting GM changes in these patients. This supports previous work in PD [54].

Visuoperceptive and visuospatial dysfunction are typical cognitive deficits of DLB [55,56] and PD [57,58], but they also feature in iRBD [16,24,53]. Research into color perception correlates in iRBD found that these abnormalities were associated with GM changes in the right cuneus and with abnormal surface expansion in the right hippocampus [48]. Additionally, lower performance in visuospatial function has been associated with thinning in the frontal, insular [48], temporal, parietal, and occipital cortices [22,48], as well as grater surface expansion in the right hippocampus [48]. Recent longitudinal work showed that a deterioration in visual discrimination over time was related to progressive reductions in bilateral superior parietal cortical regions [24]. These results agree with the visuospatial and visuoperceptive neuroanatomical correlates in PD [33,57,58].

The cognitive profile of iRBD is also frequently characterized by impairments in executive function, attention, memory, and mental processing speed [16,47,53]. Impaired attention and executive function correlate with thinning in medial superior frontal,

paracentral, sensorimotor, fusiform, lingual, and cuneus regions [48]. Lower performance in learning and memory has been associated with cortical thinning in the frontal, temporal, insular, and occipital cortices [22,48], with greater surface expansion in the right hippocampus [48] and higher thalamic-fusiform connectivity [45]. Mental processing speed has been associated with reduced functional connectivity between right superior parietal and left inferior temporal regions [47].

Impaired olfactory function has been associated with bilateral cortical thinning in lateral occipital cortices and in the right cuneus [48], orbitofrontal [22,59], and precentral regions [22]. It has also been negatively associated with ALFF in the right superior occipital gyrus [7]. Olfactory loss appears to be associated not only with changes in the olfactory circuitry but also with structural and functional posterior abnormalities consistently related to non-motor symptomatology and a worse prognosis in iRBD. Therefore, olfactory measures are highly relevant data in prodromal stages, because after an initial decline, the sense of smell will remain almost unchanged throughout the course of the synucleinopathy [24,60–62], making it a relevant biomarker of short-term conversion to either PD or DLB [63].

MRI appears sensitive to detecting the clinical and neuropsychological neural correlates of iRBD, yet studies that use functional approaches are still scarce. There is also a lack of research providing information from a longitudinal perspective, which will be necessary to associate distinct MRI markers to specific patterns of clinical progression.

Concluding remarks and future directions

There is a strong evidence that iRBD is a prodromal feature of synuclein-mediated disorders, with up to 90% converting to a clinically definable synucleinopathy after 15 years of follow-up [3]. The studies discussed in the present review indicate that structural and functional MRI can identify brain changes that progress over time in patients with iRBD and that are related to their various cognitive dysfunctions.

Most structural studies agree that there is volume reduction in the deep GM nuclei, with previous reports demonstrating a high sensitivity of cortical thickness in detecting and tracking regional cortical GM degeneration in patients with iRBD. However, most structural studies to date have been cross-sectional and carried out with small samples, necessitating large case–control studies or longitudinal studies with well-defined cases. We highlighted the interest in comparing iRBD and early PD to study a presumed aggressive phenotype of iRBD. Moreover, it would be interesting to identify patterns of cortical and subcortical involvement through more complex approaches based on data-driven and unsupervised machine learning, such as that done for other neurodegenerative disorders.

Investigations using DTI have found microstructural changes not only in GM nuclei but also in WM tissue, consistent with previous literature in neurodegenerative disorders. Despite finding WM abnormalities in iRBD, the lack of research into structural connectivity through diffusion MRI tractography is notable. Thus, much work is still to be done in this field.

Based on initial works focusing on BG functional connectivity, rs-fMRI was proposed as a promising biomarker of prodromal neurodegeneration in PD [43]. Subsequent studies have identified functional connectivity abnormalities involving not only the BG but also the cortico-striatal networks. More recent studies go beyond this circuitry, using sophisticated whole brain approaches to avoid the preselection of regions of interest. It has been shown that patients with iRBD have disrupted connectivity involving associative regions of the temporal and parietal lobes that are known to support complex cognitive functions. Several investigations have therefore shown that MRI can detect structural and functional brain changes in iRBD that correlate with motor and non-motor symptomatology. Unfortunately, there is a lack of data providing information about functional connectivity changes from a longitudinal perspective, which will be needed to associate distinct MRI markers to specific clinical progressions.

Although these complex MRI methodologies are not used routinely in clinical practice because they are uneconomical and have sophisticated preprocessing requirements, their use in research has provided notable improvements in the characterization of iRBD. Nonetheless, only one longitudinal work has aimed at investigating those specific structural MRI changes that can help in distinguishing the progression from iRBD to a clinically defined synucleinopathy, highlighting the relevance of cortical degeneration. In this sense, it is anticipated that MRI may soon be able to help with the monitoring of disease progression, and perhaps even be of use in determining the short-term risk of subsequent phenoconversion. Finally, larger case–control further research must study iRBD longitudinally, implementing multimodal imaging that uses complex approaches based on data-driven and unsupervised machine learning. This should provide greater insights into the natural course of iRBD.

Funding

This study was sponsored by the Spanish Ministry of Economy and Competitiveness ([PSI2017-86930-P] cofinanced by Agencia Estatal de Investigación (AEI) and the European Regional Development Fund), and by Generalitat de Catalunya [2017SGR748].

Author contributions

CJ conceived of the present idea. All the authors contributed to the draft of the article and revised the manuscript critically for important intellectual content and approved the final version of the manuscript.

Practice points

1) iRBD is a prodromal stage of the various clinically defined synucleinopathies. These patients typically progress to PD, DLB, and rarely, MSA.
2) The pathogenesis of RBD is thought to be related to dysfunction of the lower brainstem nuclei. Nevertheless, since iRBD is a harbinger for developing the clinical synucleinopathies, it is reasonable to expect dysfunction in other structures such as the striatum, the substantia nigra, the limbic system, and the cortex, which may indicate a widespread neurodegenerative process.
3) Structural MRI have demonstrated iRBD have deep gray matter nuclei changes, cortical gray matter atrophy and microstructural abnormalities in white matter tissue.
4) Functional MRI identified disrupted functional connectivity within the basal ganglia, the cortico-striatal networks, and cortico-cortical connectivity.
5) Investigations have shown that MRI can detect brain changes associated with the motor and non-motor symptoms of iRBD.

Research agenda

1) Investigate the natural course of iRBD with larger longitudinal case–control studies and multicentric MRI data.
2) Identify structural and functional patterns of brain degeneration through more complex approaches based on data-driven and unsupervised machine learning. With special interest in the detection of specific structural and functional patterns that can highlight patients who will convert to PD or DLB.
3) Further explore whether MRI may allow for the prediction of subsequent phenoconversion from iRBD to the clinically defined synucleinopathies.

Conflicts of interest

The authors do not have any conflicts of interest to disclose.

Appendix A. Supplementary data

Supplementary data to this article can be found online at https://doi.org/10.1016/j.smrv.2021.101495.

References

[1] Iranzo A. The REM sleep circuit and how its impairment leads to REM sleep behavior disorder. Cell Tissue Res 2018;373:245–66. https://doi.org/10.1007/s00441-018-2852-8.

[2] Iranzo A, Fairfoul G, NA-Ayudhaya A, Serradell M, Gelpi E, Vilaseca I, et al. Cerebrospinal fluid α-synuclein detection by RT-QuIC in patients with isolated rapid-eye-movement sleep behaviour disorder: a longitudinal observational study. Lancet 2021;20:203–12. https://doi.org/10.1016/S1474-4422(20)30449-X.

[3] Iranzo A, Tolosa E, Gelpi E, Molinuevo JL, Valldeoriola F, Serradell M, et al. Neurodegenerative disease status and post-mortem pathology in idiopathic rapid-eye-movement sleep behaviour disorder: an observational cohort study. Lancet Neurol 2013;12:443–53. https://doi.org/10.1016/S1474-4422(13)70056-5.

[4] Heller J, Brcina N, Dogan I, Holtbernd F, Romanzetti S, Schulz JB, et al. Brain imaging findings in idiopathic REM sleep behavior disorder (RBD) – a systematic review on potential biomarkers for neurodegeneration. Sleep Med Rev 2017;34:23–33. https://doi.org/10.1016/j.smrv.2016.06.006.

*[5] Rahayel S, Postuma RB, Montplaisir J, Bedetti C, Brambati S, Carrier J, et al. Abnormal gray matter shape, thickness, and volume in the motor cortico-subcortical loop in idiopathic rapid eye movement sleep behavior disorder: association with clinical and motor features. Cerebr Cortex 2018;28:658–71. https://doi.org/10.1093/cercor/bhx137.

*[6] Ellmore TM, Hood AJ, Castriotta RJ, Stimming EF, Bick RJ, Schiess MC. Reduced volume of the putamen in REM sleep behavior disorder patients. Park Relat Disord 2010;16:645–9. https://doi.org/10.1016/j.parkreldis.2010.08.014.

[7] Chen M, Li Y, Chen J, Gao L, Sun J, Gu Z, et al. Structural and functional brain alterations in patients with idiopathic rapid eye movement sleep behavior disorder. J Neuroradiol 2020:1–7. https://doi.org/10.1016/j.neurad.2020.04.007.

[8] Iranzo A, Santamaría J, Valldeoriola F, Serradell M, Salamero M, Gaig C, et al. Dopamine transporter imaging deficit predicts early transition to synucleinopathy in idiopathic rapid eye movement sleep behavior disorder. Ann Neurol 2017;82:419–28. https://doi.org/10.1002/ana.25026.

[9] Hanyu H, Inoue Y, Sakurai H, Kanetaka H, Nakamura M, Miyamoto T, et al. Voxel-based magnetic resonance imaging study of structural brain changes in patients with idiopathic REM sleep behavior disorder. Park Relat Disord 2012;18:136–9. https://doi.org/10.1016/j.parkreldis.2011.08.023.

[10] Park KM, Lee HJ, Lee BI, Kim SE. Alterations of the brain network in idiopathic rapid eye movement sleep behavior disorder: structural connectivity analysis. Sleep Breath 2018;23:587–93. https://doi.org/10.1007/s11325-018-1737-0.

[11] Iglesias JE, Insausti R, Lerma-Usabiaga G, Bocchetta M, Van Leemput K, Greve DN, et al. A probabilistic atlas of the human thalamic nuclei combining ex vivo MRI and histology. Neuroimage 2018;183:314–26. https://doi.org/10.1016/j.neuroimage.2018.08.012.

[12] Sabattoli F, Boccardi M, Galluzzi S, Treves A, Thompson PM, Frisoni GB. Hippocampal shape differences in dementia with Lewy bodies. Neuroimage 2008;41:699–705. https://doi.org/10.1016/j.neuroimage.2008.02.060.

[13] Delli Pizzi S, Franciotti R, Bubbico G, Thomas A, Onofrj M, Bonanni L. Atrophy of hippocampal subfields and adjacent extrahippocampal structures in dementia with Lewy bodies and Alzheimer's disease. Neurobiol Aging 2016;40:103–9. https://doi.org/10.1016/j.neurobiolaging.2016.01.010.

[14] Ibarretxe-Bilbao N, Ramírez-Ruiz B, Tolosa E, Martí MJ, Valldeoriola F, Bargalló N, et al. Hippocampal head atrophy predominance in Parkinson's disease with hallucinations and with dementia. J Neurol 2008;255:1324–31.

*[15] Scherfler C, Frauscher B, Schocke M, Iranzo A, Gschliesser V, Seppi K, et al. White and gray matter abnormalities in idiopathic rapid eye movement sleep behavior disorder: a diffusion-tensor imaging and voxel-based morphometry study. Ann Neurol 2011;69:400–7. https://doi.org/10.1002/ana.22245.

[16] Campabadal A, Segura B, Junque C, Serradell M, Abos A, Uribe C, et al. Cortical gray matter and hippocampal atrophy in idiopathic rapid eye movement sleep behavior disorder. Front Neurol 2019;10:1–9. https://doi.org/10.3389/fneur.2019.00312.

[17] Chow N, Aarsland D, Honarpisheh H, Beyer MK, Somme JH, Elashoff D, et al. Comparing hippocampal atrophy in alzheimer's dementia and dementia with lewy bodies. Dement Geriatr Cognit Disord 2012;34:44–50. https://doi.org/10.1159/000339727.

[18] Pereira JB, Junqué C, Bartrés-Faz D, Ramírez-Ruiz B, Marti M-J, Tolosa E. Regional vulnerability of hippocampal subfields and memory deficits in Parkinson's disease. Hippocampus 2013;23:720–8. https://doi.org/10.1002/hipo.22131.

[19] Li G, Chen Z, Zhou L, Zhao A, Niu M, Li Y, et al. Altered structure and functional connectivity of the central autonomic network in idiopathic rapid eye movement sleep behaviour disorder. J Sleep Res 2020. https://doi.org/10.1111/jsr.13136.

[20] Sclocco R, Beissner F, Bianciardi M, Polimeni JR, Napadow V. Challenges and opportunities for brainstem neuroimaging with ultrahigh field MRI. Neuroimage 2018;168:412–26. https://doi.org/10.1016/j.neuroimage.2017.02.052.

[21] Holtbernd F, Romanzetti S, Oertel WH, Knake S, Sittig E, Heidbreder A, et al. Convergent patterns of structural brain changes in rapid eye movement sleep behavior disorder and Parkinson's disease on behalf of the German rapid eye movement sleep behavior disorder study group. Sleep 2020:1–12. https://doi.org/10.1093/sleep/zsaa199.

*[22] Pereira JB, Weintraub D, Chahine L, Aarsland D, Hansson O, Westman E. Cortical thinning in patients with REM sleep behavior disorder is associated with clinical progression. Npj Park Dis 2019;3(5):7. https://doi.org/10.1038/s41531-019-0079-3.

[23] Rahayel S, Montplaisir J, Monchi O, Bedetti C, Postuma RB, Brambati S, et al. Patterns of cortical thinning in idiopathic rapid eye movement sleep behavior disorder. Mov Disord 2015;30:680–7. https://doi.org/10.1002/mds.25820.

*[24] Campabadal A, Inguanzo A, Segura B, Serradell M, Abos A, Uribe C, et al. Cortical gray matter progression in idiopathic REM sleep behavior disorder and its relation to cognitive decline. NeuroImage Clin 2020;28:102421. https://doi.org/10.1016/j.nicl.2020.102421.

[25] Uribe C, Segura B, Baggio HC, Abos A, Garcia-Diaz AI, Campabadal A, et al. Progression of Parkinson's disease patients' subtypes based on cortical thinning: 4-year follow-up. Parkinsonism Relat Disord 2019;64:286–92. https://doi.org/10.1016/j.parkreldis.2019.05.012.

[26] Uribe C, Segura B, Baggio HC, Abos A, Marti MJ, Valldeoriola F, et al. Patterns of cortical thinning in nondemented Parkinson's disease patients. Mov Disord 2016;31:699–708. https://doi.org/10.1002/mds.26590.

[27] Whitwell JL, Przybelski SA, Weigand SD, Ivnik RJ, Vemuri P, Gunter JL, et al. Distinct anatomical subtypes of the behavioural variant of frontotemporal dementia: a cluster analysis study. Brain 2009;132:2932–46. https://doi.org/10.1093/brain/awp232.

[28] Abós A, Baggio HC, Segura B, García-Díaz AI, Compta Y, Martí MJ, et al. Discriminating cognitive status in Parkinson's disease through functional connectomics and machine learning. Sci Rep 2017;7:1–13. https://doi.org/10.1038/srep45347.

[29] Inguanzo A, Sala-llonch R, Segura B, Erostarbe H, Abos A. Parkinsonism and Related Disorders Hierarchical cluster analysis of multimodal imaging data identifies brain atrophy and cognitive patterns in Parkinson ' s disease. Park Relat Disord 2021;82:16–23. https://doi.org/10.1016/j.parkreldis.2020.11.010.

[30] Muñoz-Lopetegi A, Berenguer J, Iranzo A, Serradell M, Pujol T, Gaig C, et al. Magnetic resonance imaging abnormalities as a marker of multiple system atrophy in isolated rapid eye movement sleep behavior disorder. Sleep 2020:1–9. https://doi.org/10.1093/sleep/zsaa089.

[31] Delli Pizzi S, Franciotti R, Tartaro A, Caulo M, Thomas A, Onofrj M, et al. Structural alteration of the dorsal visual network in DLB patients with visual hallucinations: a cortical thickness MRI study. PloS One 2014;9:e86624. https://doi.org/10.1371/journal.pone.0086624.

[32] Ramírez-Ruiz B, Martí M-J, Tolosa E, Giménez M, Bargalló N, Valldeoriola F, et al. Cerebral atrophy in Parkinson's disease patients with visual hallucinations. Eur J Neurol 2007;14:750–6. https://doi.org/10.1111/j.1468-1331.2007.01768.x.

[33] Segura B, Baggio HC, Marti MJ, Valldeoriola F, Compta Y, Garcia-Diaz AI, et al. Cortical thinning associated with mild cognitive impairment in

* The most important references are denoted by an asterisk.

Parkinson's disease. Mov Disord 2014;29:1495–503. https://doi.org/10.1002/mds.25982.
*[34] Unger MM, Belke M, Menzler K, Heverhagen JT, Keil B, Stiasny-Kolster K, et al. Diffusion tensor imaging in idiopathic REM sleep behavior disorder reveals microstructural changes in the brainstem, substantia nigra, olfactory region, and other brain regions. Sleep 2010;33:767–73. https://doi.org/10.1093/sleep/33.6.767.
[35] Pyatigorskaya N, Gaurav R, Arnaldi D, Leu-Semenescu S, Yahia-Cherif L, Valabregue R, et al. Magnetic resonance imaging biomarkers to assess substantia nigra damage in idiopathic rapid eye movement sleep behavior disorder. Sleep 2017;40. https://doi.org/10.1093/sleep/zsx149.
[36] Ohlhauser L, Smart CM, Gawryluk JR. Tract-based spatial statistics reveal lower white matter integrity specific to idiopathic rapid eye movement sleep behavior disorder as a proxy for prodromal Parkinson's disease. J Parkinsons Dis 2019;9:723–31. https://doi.org/10.3233/JPD-191688.
[37] Filippi M, Agosta F. Diffusion tensor imaging and functional MRI. 1st ed., vol. 136. Elsevier B.V.; 2016. https://doi.org/10.1016/B978-0-444-53486-6.00056-9.
[38] Wen MC, Heng HSE, Hsu JL, Xu Z, Liew GM, Au WL, et al. Structural connectome alterations in prodromal and de novo Parkinson's disease patients. Park Relat Disord 2017;45:21–7. https://doi.org/10.1016/j.parkreldis.2017.09.019.
[39] Peña-Nogales Ó, Ellmore TM, De Luis-García R, Suescun J, Schiess MC, Giancardo L. Longitudinal connectomes as a candidate progression marker for prodromal Parkinson's disease. Front Neurosci 2019;13:1–13. https://doi.org/10.3389/fnins.2018.00967.
[40] Alexander-Bloch A, Giedd JN, Bullmore E. Imaging structural co-variance between human brain regions. Nat Rev Neurosci 2013;14:322–36. https://doi.org/10.1038/nrn3465.
*[41] Rolinski M, Griffanti L, Piccini P, Roussakis AA, Szewczyk-Krolikowski K, Menke RA, et al. Basal ganglia dysfunction in idiopathic REM sleep behaviour disorder parallels that in early Parkinson's disease. Brain 2016;139:2224–34. https://doi.org/10.1093/brain/aww124.
*[42] Ellmore TM, Castriotta RJ, Hendley KL, Aalbers BM, Furr-Stimming E, Hood AJ, et al. Altered nigrostriatal and nigrocortical functional connectivity in rapid eye movement sleep behavior disorder. Sleep 2013;36:1885–92. https://doi.org/10.5665/sleep.3222.
[43] Postuma RB. Resting state MRI: a new marker of prodromal neurodegeneration? Brain 2016;139:2104–12. https://doi.org/10.1093/brain/aww131.
[44] Dayan E, Browner N. Alterations in striato-thalamo-pallidal intrinsic functional connectivity as a prodrome of Parkinson's disease. NeuroImage Clin 2017;16:313–8. https://doi.org/10.1016/j.nicl.2017.08.003.
[45] Byun J-I, Kim H-W, Kang H, Cha KS, Sunwoo J-S, Shin J-W, et al. Altered resting-state thalamo-occipital functional connectivity is associated with cognition in isolated rapid eye movement sleep behavior disorder. Sleep Med 2020;69:198–203. https://doi.org/10.1016/j.sleep.2020.01.010.
[46] Li G, Chen Z, Zhou L, Yao M, Luo N, Kang W, et al. Abnormal intrinsic brain activity of the putamen is correlated with dopamine deficiency in idiopathic rapid eye movement sleep behavior disorder. Sleep Med 2020;75:73–80. https://doi.org/10.1016/j.sleep.2019.09.015.
*[47] Campabadal A, Abos A, Segura B, Serradell M, Uribe C, Baggio HC, et al. Disruption of posterior brain functional connectivity and its relation to cognitive impairment in idiopathic REM sleep behavior disorder. NeuroImage Clin 2020;25:102138. https://doi.org/10.1016/j.nicl.2019.102138.
*[48] Rahayel S, Postuma RB, Montplaisir J, Génier Marchand D, Escudier F, Gaubert M, et al. Cortical and subcortical gray matter bases of cognitive deficits in REM sleep behavior disorder. Neurology 2018;90:e1759–70. https://doi.org/10.1016/S0306-4522(99)00316-4.
[49] Compta Y, Valente T, Saura J, Segura B, Iranzo Á, Serradell M, et al. Correlates of cerebrospinal fluid levels of oligomeric- and total-α-synuclein in premotor, motor and dementia stages of Parkinson's disease. J Neurol 2015;262:294–306. https://doi.org/10.1007/s00415-014-7560-z.
[50] Bourgouin P, Rahayel S, Gaubert M, Postuma RB. Parkinsonism and Related Disorders Gray matter substrates of depressive and anxiety symptoms in idiopathic REM sleep behavior disorder. Park Relat Disord 2018. https://doi.org/10.1016/j.parkreldis.2018.12.020. 0–1.
[51] Yamada G, Ueki Y, Oishi N, Oguri T, Fukui A, Nakayama M, et al. Nigrostriatal dopaminergic dysfunction and altered functional connectivity in rem sleep behavior disorder with mild motor impairment. Front Neurol 2019;10:1–12. https://doi.org/10.3389/fneur.2019.00802.
[52] Ehgoetz Martens KA, Matar E, Shine JM, Phillips JR, Georgiades MJ, Grunstein RR, et al. The neural signature of impaired dual-tasking in idiopathic rapid eye movement sleep behavior disorder patients. Mov Disord 2020;35:1596–606. https://doi.org/10.1002/mds.28114.
[53] Högl B, Stefani A, Videnovic A. Idiopathic REM sleep behaviour disorder and neurodegeneration - an update. Nat Rev Neurol 2018;14:40–56. https://doi.org/10.1038/nrneurol.2017.157.
[54] Pereira JB, Ibarretxe-Bilbao N, Marti M-J, Compta Y, Junqué C, Bargallo N, et al. Assessment of cortical degeneration in patients with Parkinson's disease by voxel-based morphometry, cortical folding, and cortical thickness. Hum Brain Mapp 2012;33:2521–34. https://doi.org/10.1002/hbm.21378.
[55] Levy JA, Chelune GJ. Cognitive-behavioral profiles of neurodegenerative dementias: beyond alzheimer's disease. J Geriatr Psychiatr Neurol 2007;20:227–38. https://doi.org/10.1177/0891988707308806.
[56] Tiraboschi P, Salmon DP, Hansen LA, Hofstetter RC, Thal LJ, Corey-Bloom J. What best differentiates Lewy body from Alzheimer's disease in early-stage dementia? Brain 2006;129:729–35. https://doi.org/10.1093/brain/awh725.
[57] Pereira JB, Junqué C, Martí M-J, Ramirez-Ruiz B, Bargalló N, Tolosa E. Neuroanatomical substrate of visuospatial and visuoperceptual impairment in Parkinson's disease. Mov Disord 2009;24:1193–9. https://doi.org/10.1002/mds.22560.
[58] Garcia-Diaz AI, Segura B, Baggio HC, Marti MJ, Valldeoriola F, Compta Y, et al. Structural brain correlations of visuospatial and visuoperceptual tests in Parkinson's disease. J Int Neuropsychol Soc 2018;24:33–44. https://doi.org/10.1017/S1355617717000583.
[59] Campabadal A, Segura B, Junque C, Serradell M, Abos A, Uribe C, et al. Comparing the accuracy and neuroanatomical correlates of the UPSIT-40 and the Sniffin' Sticks test in REM sleep behavior disorder. Park Relat Disord 2019;65:197–202. https://doi.org/10.1016/j.parkreldis.2019.06.013.
[60] Campabadal A, Uribe C, Segura B, Baggio HC, Abos A, Garcia-Diaz AI, et al. Brain correlates of progressive olfactory loss in Parkinson's disease. Park Relat Disord 2017;41:44–50. https://doi.org/10.1016/j.parkreldis.2017.05.005.
[61] Herting B, Schulze S, Reichmann H, Haehner A, Hummel T. A longitudinal study of olfactory function in patients with idiopathic Parkinson's disease. J Neurol 2008;255:367–70. https://doi.org/10.1007/s00415-008-0665-5.
[62] Iranzo A, Serradell M, Vilaseca I, Valldeoriola F, Salamero M, Molina C, et al. Longitudinal assessment of olfactory function in idiopathic REM sleep behavior disorder. Park Relat Disord 2013;19:600–4. https://doi.org/10.1016/j.parkreldis.2013.02.009.
[63] Iranzo A, Marrero-González P, Serradell M, Gaig C, Santamaria J, Vilaseca I. Significance of hyposmia in isolated REM sleep behavior disorder. J Neurol 2020. https://doi.org/10.1007/s00415-020-10229-3.
[64] Lee JH, Han YH, Cho JW, Lee JS, Lee SJ, Kim DJ, et al. Evaluation of brain iron content in idiopathic REM sleep behavior disorder using quantitative magnetic resonance imaging. Park Relat Disord 2014;20:776–8. https://doi.org/10.1016/j.parkreldis.2014.03.023.